Research Article

Modeling of Forklift Drivetrain and Test Verification of Fuel Consumption

Orkan Buran[1*], Ali Can Tellioğlu[2], Mustafa Demir[3], Hüseyin Samet Kartal[4]

[1] Tümosan Teknoloji Mühendislik Sanayi Ticaret Anonim Şirketi, Orcid ID: https://orcid.org/0000-0003-3384-283X,E-mail: orkan.buran@tumosanmuhendislik.com.tr
[2] Tümosan Teknoloji Mühendislik Sanayi Ticaret Anonim Şirketi, Orcid ID: https://orcid.org/ 0000-0003-0181-0921, E-mail: alican.tellioglu@tumosanmuhendislik.com.tr
[3] Tümosan Teknoloji Mühendislik Sanayi Ticaret Anonim Şirketi, Orcid ID: https://orcid.org/0009-0001-2830-7894, E-mail: mustafa.demir@tumosanmuhendislik.com.tr
[4] Tümosan Teknoloji Mühendislik Sanayi Ticaret Anonim Şirketi, Orcid ID: https://orcid.org/0009-0006-1682-2940, E-mail: samet.kartal@tumosanmuhendislik.com.tr
[*] Correspondence: orkan.buran@tumosanmuhendislik.com.tr

Received 13 October 2024
Received in revised form 28 November 2024
In final form 18 December 2024

Reference: Buran, O., Tellioğlu, A. C., Demir, M., & Kartal, H. S. (2024). Modeling of forklift drivetrain and test verification of fuel consumption. The European Journal of Research and Development, 4(4), 127-164.

Abstract

Fuel consumption values of all used vehicles, whether they are construction machines or stacking machines, need to be calculated or convergently determined at the drafting stage. In this study, all parameters affecting the fuel consumption of a forklift truck are modeled in a computer environment and then this forklift truck is tested according to the fuel consumption part of VDI 2198 and the model and test data are compared. As a result of this study, we will have a fuel consumption model validated with test data and we will know the fuel consumption value without the need for testing in future forklift operations.

Keywords: *VDI 2198, Forklift Truck, Fuel Consumption,*

1. Introduction

In order to determine and optimize the fuel consumption of a forklift truck, there are some basic components to be intervened in the design phase. These are the engine, gearbox, torque converter, overall gear ratios, wheel diameter and vehicle dimensions. Apart from these basic components, the curb weight of the truck is also a very important parameter. With the forklift fuel consumption model to be validated, changes will be

made to the components and elements mentioned above and their effects on fuel consumption will be observed.

The general view of the forklift truck, which is also the subject of this study, is shown in Figure 1.

Figure 1: General View of Forklift Truck

2. Materials and Methods

2.1. Key Characteristics of The Forklift Truck

In this study, TMSN ALF forklift truck with 3500 kg payload capacity will be used. The basic vehicle specifications of this forklift are shown in Table 1.

Table 1: Basic Specifications of Forklift Truck

No	Description		Unit	Value
1	Vehicle Weight	Loaded	kg	8584
2		Unloaded	kg	5084
3	Engine Model		-	3DN-29T-048C
4	Maximum Power		kW	36 @ 2400 rpm
5			HP	48 @ 2400 rpm
6	Effective Wheel Radius	Loaded	mm	318
7		Unloaded	mm	346
8	Vehicle Projection Area		m2	2,7
9	Coefficient of Aerodynamic Resistance (CD)		-	0,8
10	Rolling Resistance Coefficient		-	0,01

The vital parts that make up a diesel forklift are shown in Figure 2.

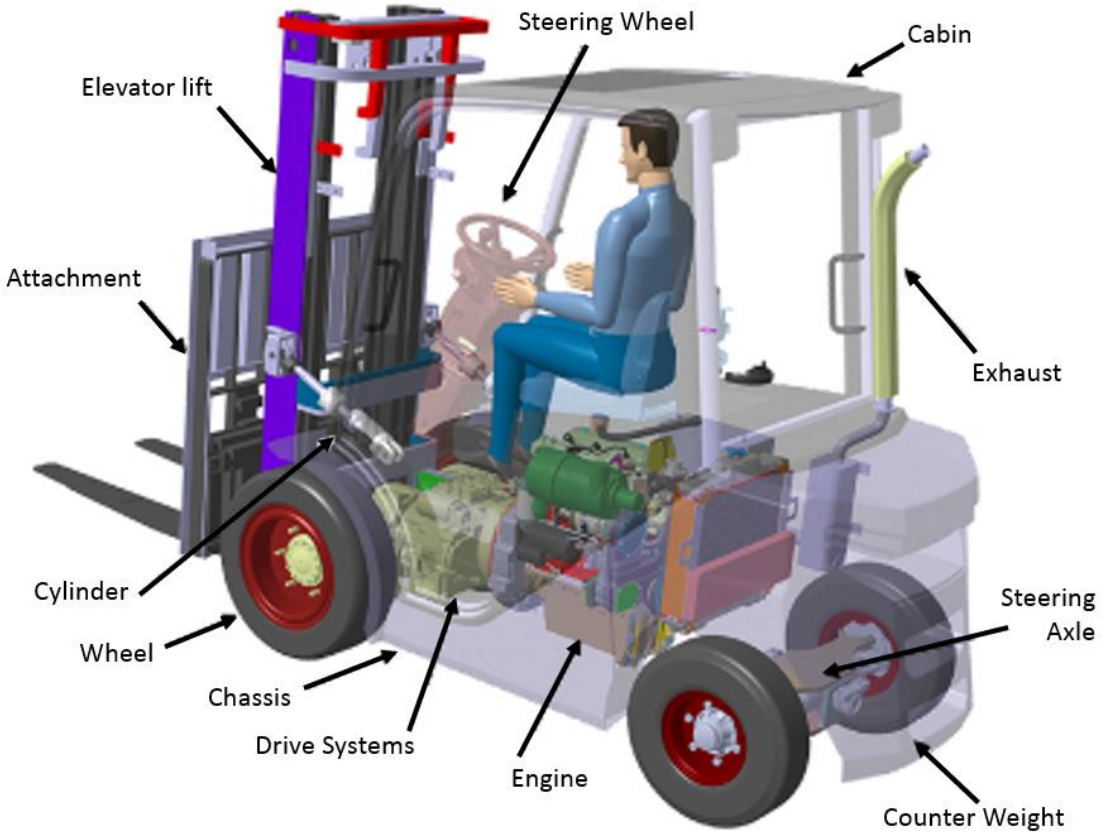

Figure 2: Vital Parts of Forklifts

2.2. Diesel Engine

The main features of the S8000 coded Tümosan engine used in the forklift, which is the subject of this study, are as shown in Table 2.

Table 2: Features of Diesel Engine [2]

Model	**3DN-29T-048C**
Cylinder Layout	inline
Rated Power @ 2300 rpm	48 Hp
Rated Torque @ 1500 rpm	170 Nm
Total Engine Capacity	2908 cm^3
Diameter x Stroke	104 mm x 115 mm
Number of Cylinder	3

Minimum Specic Fuel Consumption	160 g/Hph
Aspiration	Natural Emission
Number of valves per cylinder	2
Compression Ratio	17:1
Dry weight	300 kg
Wet weight	325 kg
Emission Level	Stage III A
Injection type	Mechanical injection
Cooling System	Water-cooled

The power and torque curves of Tümosan brand diesel engine coded 3DN-29T-048C are as shown in Figure 3.

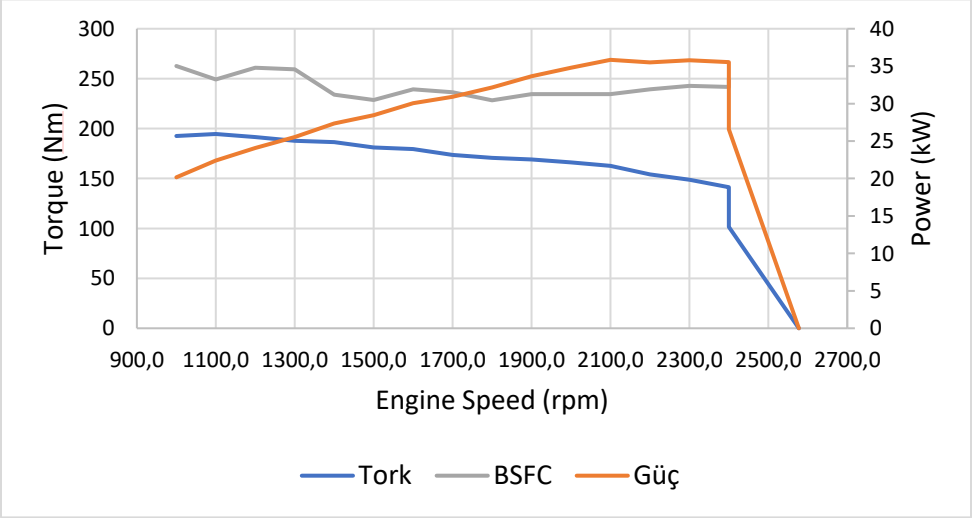

Figure 3: Engine Performance Curves [2]

2.3. Propulsion System

The propulsion systems used in forklifts are classified according to different structural configurations, mainly Mechanical, Hydrodynamic and Hydrostatic systems. The forklift drive system considered in this study is a Mechanical System. One of the most important advantages of this system is the use of a gear pump in the hydraulic system of the load carrying mechanism. Since it is a constant capacity pump, a consistent amount of oil flow is provided depending on the engine speed, regardless of whether the load handling system is running or not [3].

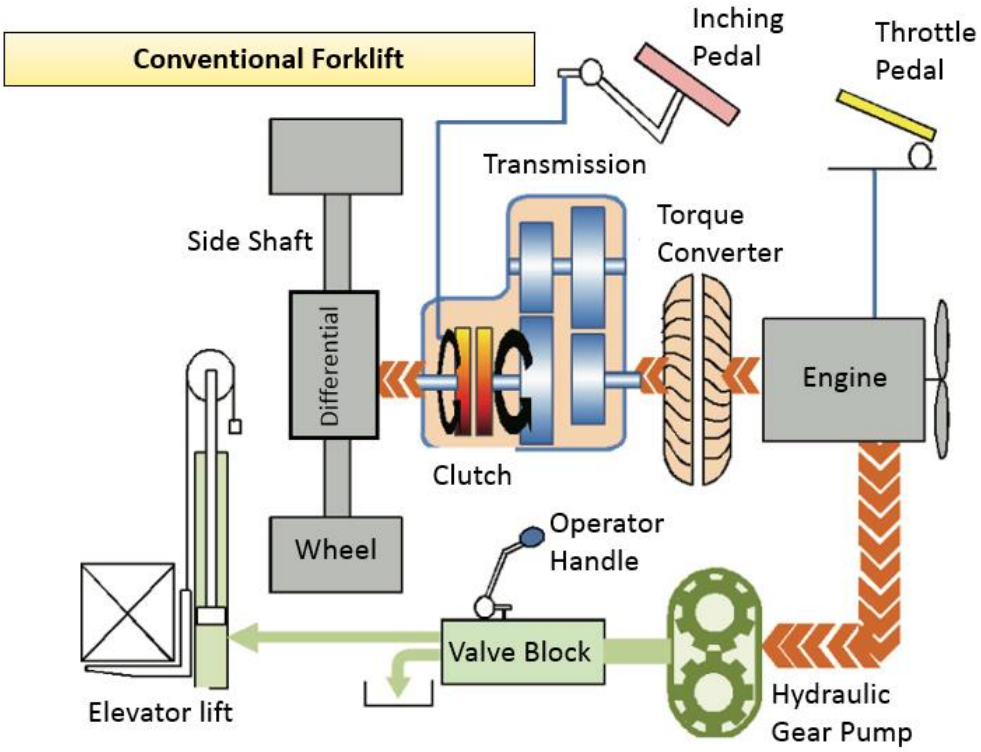

Figure 4: Generic Scheme Diagram of a Mechanical Forklift Truck [3]

The working structure of the mechanical forklift is shown in figure 4. In summary, it consists of a diesel engine, a torque-converted transmission, a differential in the front axle and a wheel. Also shown is a hydraulic pump powered by the diesel engine.

2.4. Gearbox With Torque Converter

In this forklift truck; TNA brand transmission with torque converter, 1 forward and 1 reverse gearbox was used. The technical specifications of this transmission are shown in Table 3.

Table 3 General features of the transmission [4]

Transmission Brand	Hyundai
Transmission Model	HT30-TS010
Maximum Input Power (kW)	55
Maximum Input Torque (Nm)	620
Type	Full Floated & Power Shift
Torque Converter Type	1 Stage – 2 Phase
Torque Converter Stall Ratio	2,87
Gear Ratio	1,438

The performance curves of the torque converter are also as shown in figure 5 below.

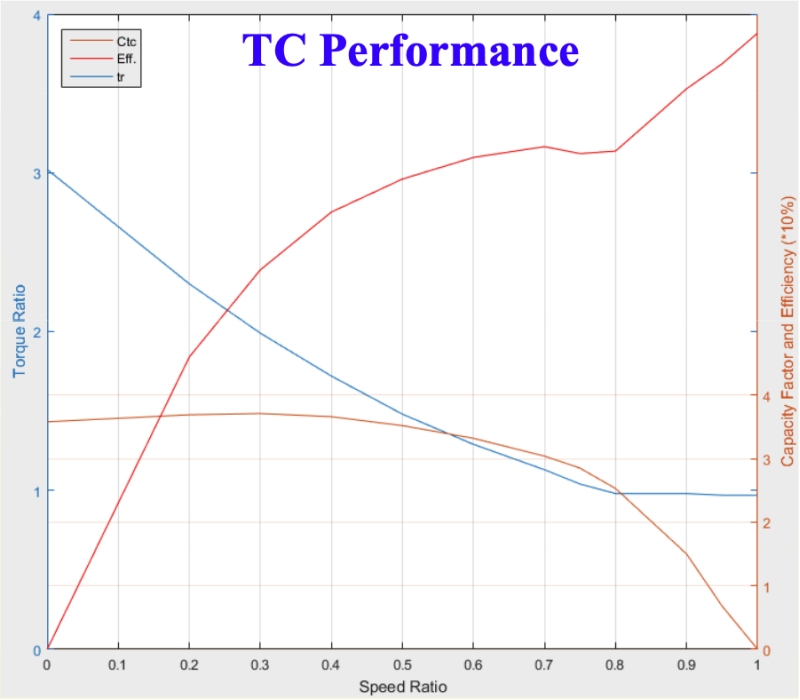

Figure 5: Torque Convertor Performance Curve [4]

2.5. Traction Axle

The power from the transmission enters the differential located inside the traction axle to be distributed to the right and left wheels, where the power separated as right and left enters the hub reducers through the side axles and the power is transferred to the road through the wheels. The component that contains this differential, side shafts and hub reducer is called the drive hanger.

A representative cross-sectional view of this traction axle is shown in figure 6.

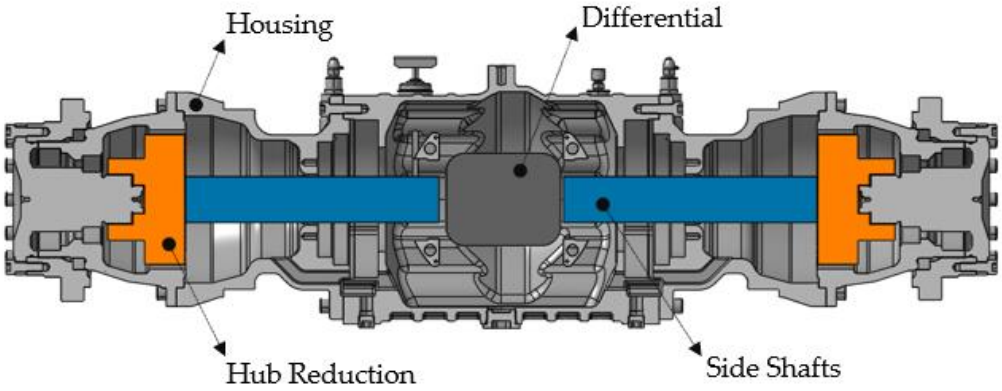

Figure 6: Cross-Sectional View of The Traction Axle [5]

The main features of this traction axle are as shown in Table 4.

Table 4: Traction Axle Characteristics [4]

Traction Axle Name	TNA
Traction Axle No	HA30-TS010
Max. Input Torque (Nm)	620
Differential Gear Ratio	2,818
Hub Reduction Gear Ratio	4,105

2.6. Power Demand

For the vehicle to move, the movement condition must be satisfied. Assuming no slip occurs between the wheel and the road, the required power can be represented as follows.

$$N_e = \frac{\sum W . V_{vehicle}}{\mu_m}$$

2.7. Resistances Affecting the Vehicle

The forces opposing the motion of a vehicle, acting along the vehicle's axis, are collectively referred to as motion resistances [6]. To achieve the motion condition, the required power must exceed these resistances. Accurately determining the total resistances acting on the vehicle is crucial, as it ensures a precise evaluation of the vehicle's performance capabilities.

Table 5: Total Movement Resistances Acting on a Vehicle [6]

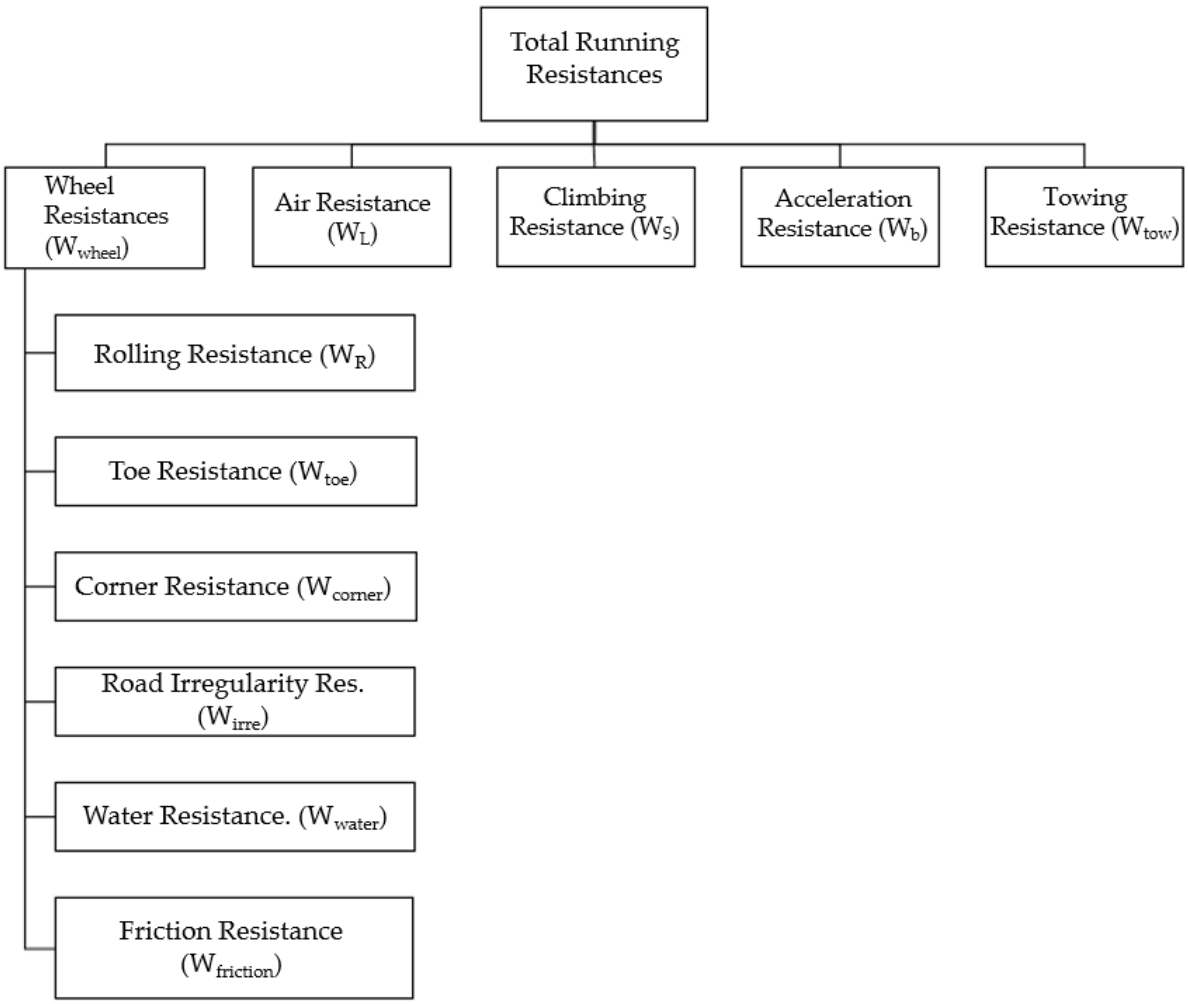

The total resistances acting on the vehicle are shown in the equation below;

$$\sum W = W_R + W_L + W_S + W_B$$

The detailed representation of the total resistances is provided in the equation below; [6]

$$\Sigma W = f_0 \cdot \left(1 + \frac{\left(\frac{V_T}{3.6}\right)^2}{1500} \right) .G.\cos\alpha + \frac{1}{2}.\rho_h.C_D.A.V^2 + G.\mathrm{Sin}\alpha + \varphi.m.\frac{dV_T}{dt} + W_Ç$$

2.8. Test Cycle

In this research, the fuel consumption of the forklift will be assessed based on the VDI 2198 cycle. The primary reason for using the VDI 2198 standard is its widespread acceptance within the industry, as fuel consumption values in forklift catalogs are typically specified according to this standard. The dimensions of the fuel consumption cycle depicted in Figure 7 of VDI 2198 differ depending on the vehicle type. The fuel consumption track will be adapted for the forklift, specifically considering the "Counterweight Lifting Truck" type outlined in Table 6

Table 6: Dimensions of the fuel consumption test track according to forklift types according to VDI 2198 [7]

Table 3. Comparison of the industrial truck types

	Electric counter-weight lift truck with seated operator > 1,6 t and all i.c.-lift trucks	Electric fork-lift truck ≤ 1,6 t	Reachtruck with seated/ standing operator	Pallet stacking trucks and other high-lift trucks	Pallet trucks and other lift trucks	Fixed-platform trucks, tractors
No. of cycles/h	60	45[a)]	35	20	20	80
Distance *L*, in m	30	30	30	30	30	50
Lift at A an B, in m	2	2	4	2	0,1	

[a)] Notice: For high-performance electric trucks below 1,6 t, 60 cycles are also permissible, provided that the amount of cycles is noted in line 6.6 of Table1.

A general illustration of the road loop, where the dimensions outlined in Table 6 are to be implemented, is presented in Figure 7.

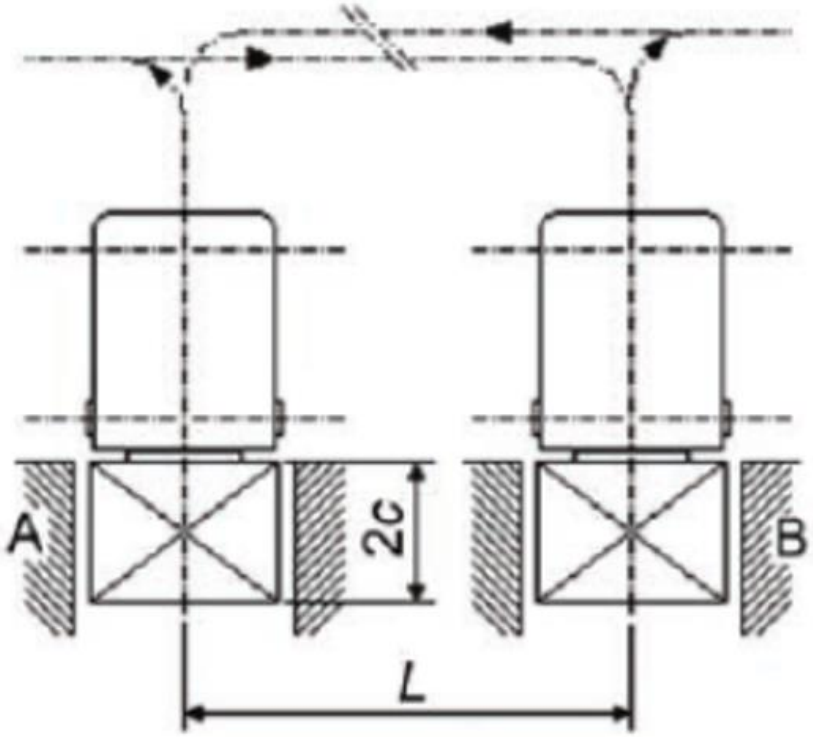

Figure 7: Sketch of the fuel consumption track according to VDI 2198

When a fuel consumption cycle is created following the sketch in Figure 7 and the dimensions provided in Table 6, the track depicted in Figure 8 is obtained. This track is designed around the load handling zones labeled A and B, which are separated by a 30-meter distance. The goal is to simulate a fuel consumption cycle where the forklift reaches point A, raises its load by 2 meters, lowers the load, proceeds to point B, repeats the lifting and lowering process by 2 meters, and then returns to point A. This sequence is continuously repeated for a duration of 60 minutes.

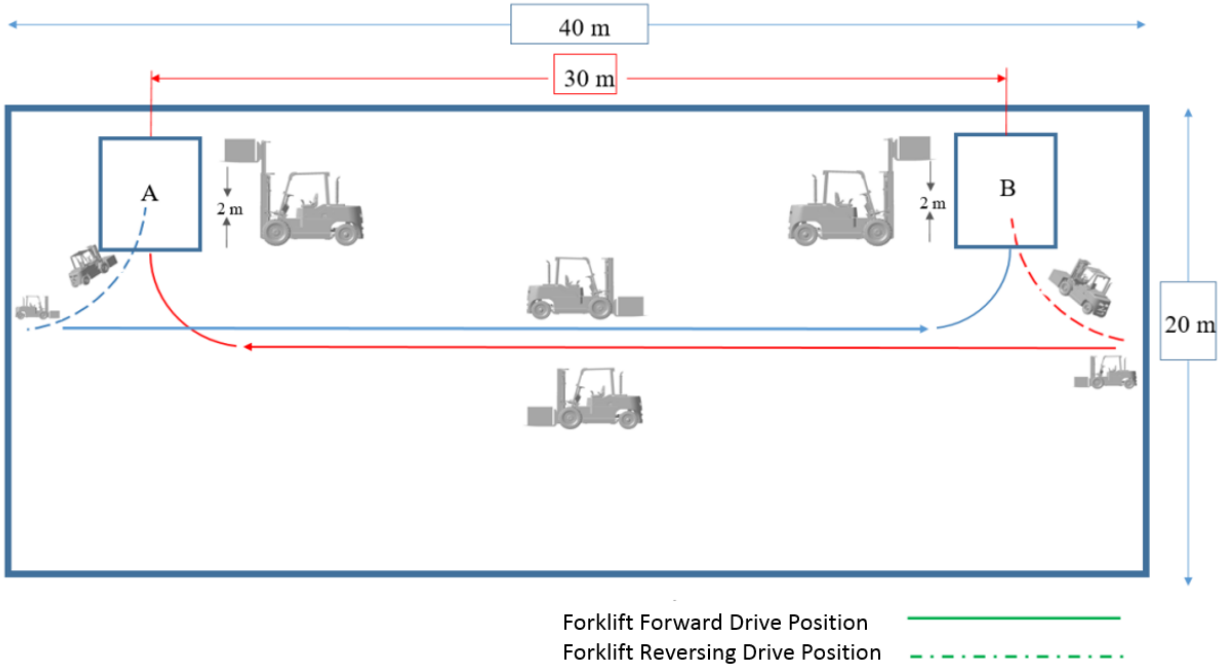

Figure 8: Test Cycle According to VDI 2198 [8]

2.9. Test Conditions

Before starting the test, all fluids of the test forklift (fuel and hydraulic system oil), as well as the tire pressures and tread depths, were checked as illustrated in Figure 9.

Figure 9: Checking the Depth of The Front and Rear Tires

The test track defined by the VDI 2198 standard was implemented as shown in Figure 10.

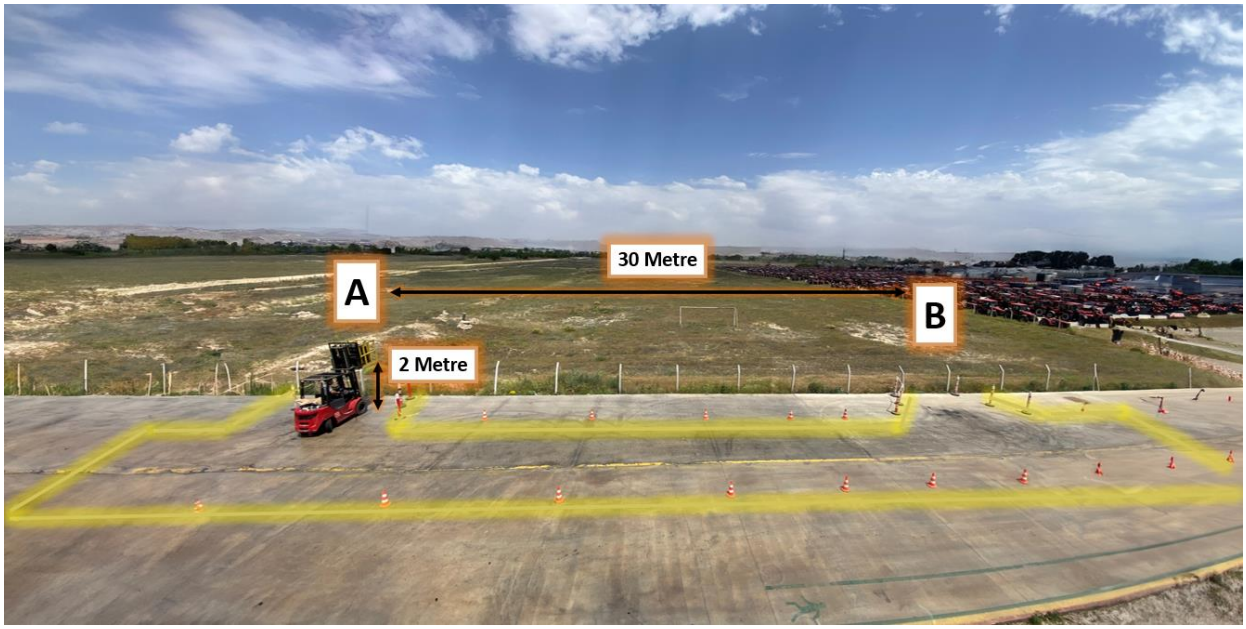

Figure 10: Test Area

In accordance with the requirement outlined in VDI 2198 to lift the load to a height of 2 meters, a marker has been placed on the lift system, as illustrated in Figure 11. This allows the operator to perform the lifting operation efficiently and accurately stop the load precisely at the 2-meter height during testing.

Figure 11: Elevation Limit Adjustment

Before starting the test, the forklift was fully prepared by filling all fluids, equipping it with the necessary test apparatus and loading a controlled test weight. The forklift was weighed at the weighbridge in Tümosan Konya factory and its test-ready weight was recorded as 8440 kg. Including the weight of the test operator, the total test weight was 8510 kg. The position of the truck on the weighbridge is shown in Figure 12.

Figure 12: Weight Measurement

2.10. Road Testing

During road tests, the forklift will require two main sources of power. The first is the energy transferred from the engine to the wheels via the drivetrain, enabling the forklift's movement. The second power requirement is for the lifting mechanism, driven by a hydraulic oil pump connected to the transmission PTO. To measure the first power demand, a strain gauge was installed on the intermediate shaft positioned between the transmission and the drive axle.

Figure 13: Strain Gage Adapted to The Center Shaft

A wireless transmitter and power source, mounted on the rotating intermediate shaft, were used to transfer data from the strain gauge to the telemetry system. The setup, including the transmitter and power source fixed to the intermediate shaft, is depicted in Figure 13.

Figure 14: Transmitter Module and Power Supply for Wireless Measurement

The installation of the previously mentioned strain gauge, transmitter module, and power source on the intermediate shaft of the vehicle is shown in Figure 14.

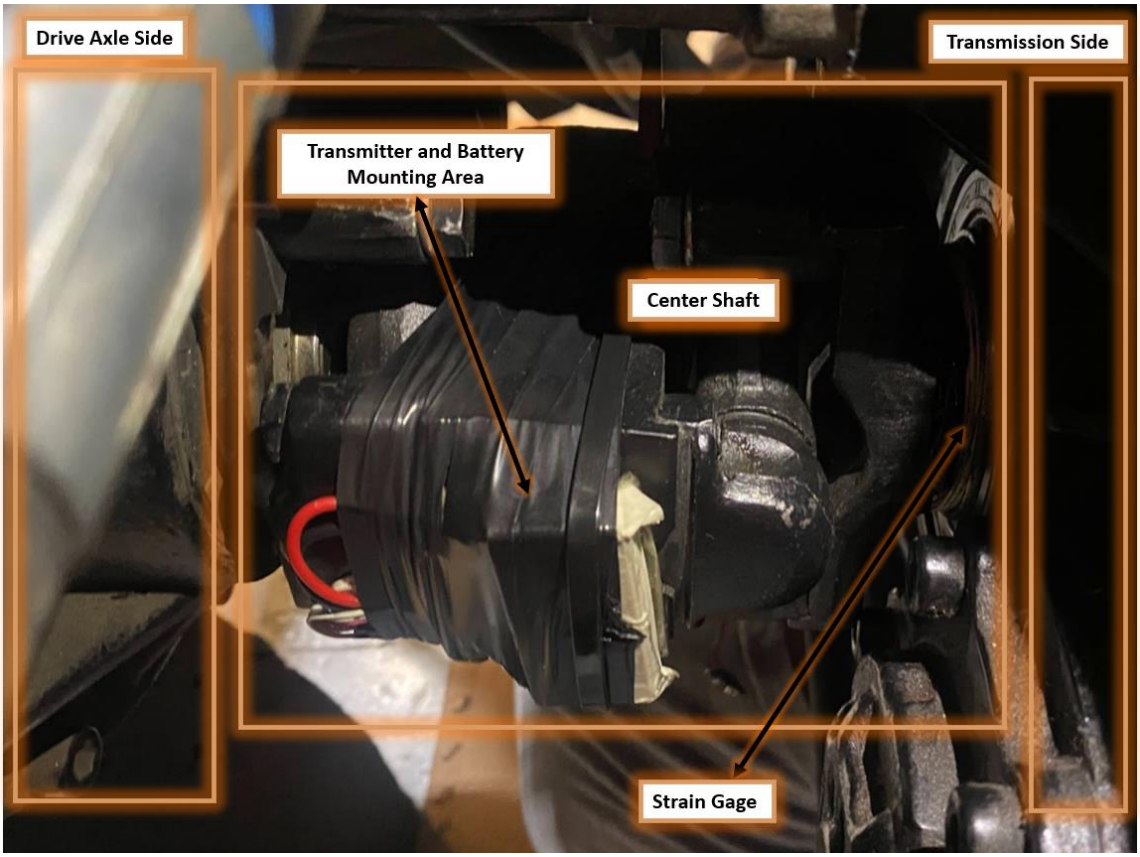

Figure 15: Position of the Center Shaft On The Truck Where The Strain Gage And Transmitter Are Instrumented

The deformation occurring on the shaft is measured using the strain gauge and transmitted to the telemetry system, shown in Figure 16, in mV/V format.

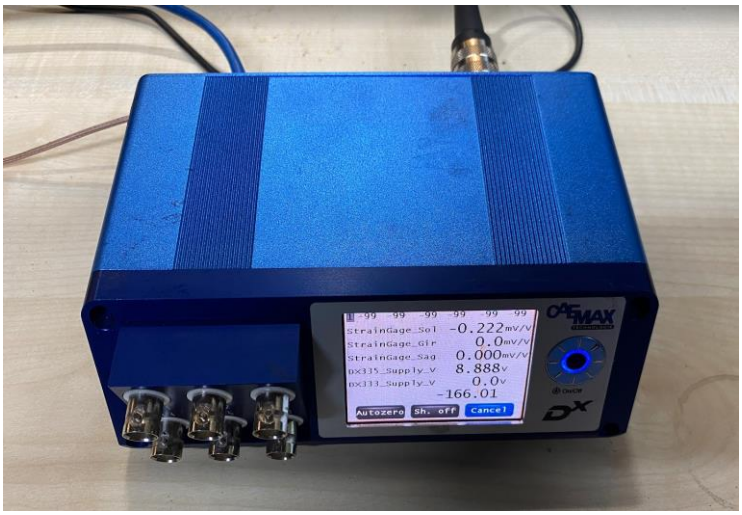

Figure 16: Modular multichannel telemetry system

The flowmeter, mounted at the oil pump outlet (where the pressure line begins) to measure the power consumption of the oil pump, representing the second power demand, is depicted in Figure 17.

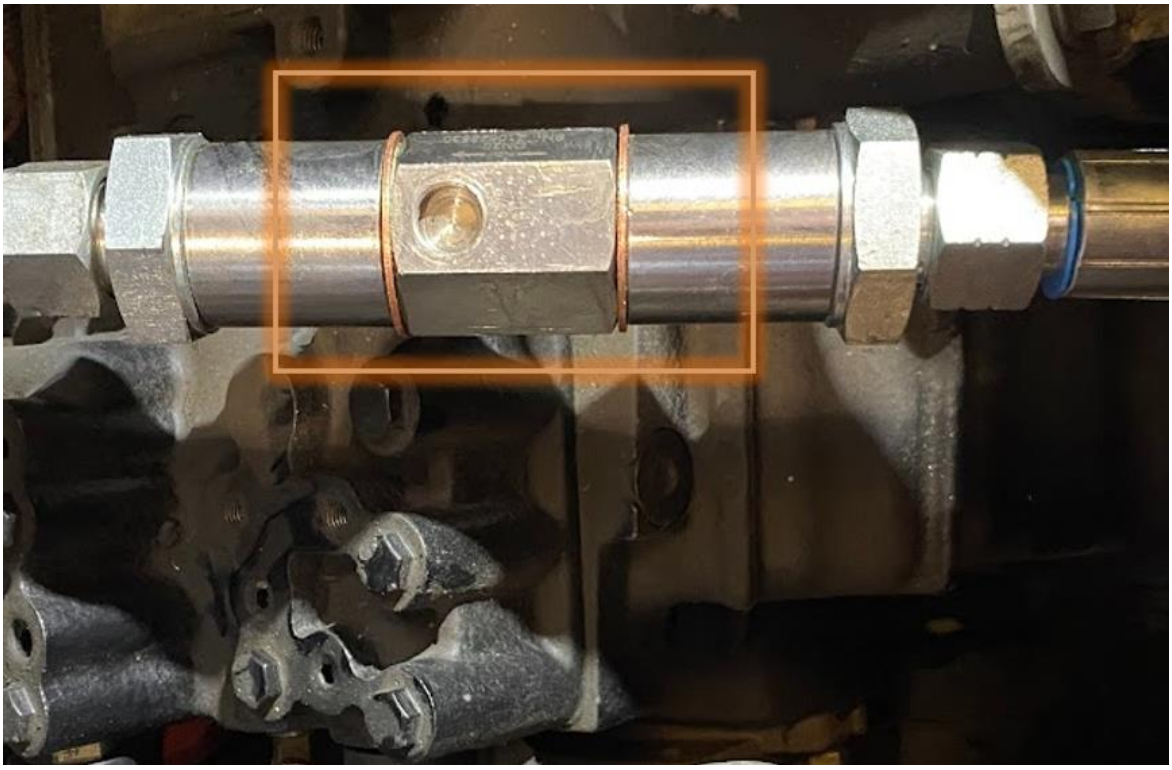

Figure 17: Flow Meter Installed in The Pressure Line of The Oil Pump

The image of the pressure gauge installed at the oil pump outlet for the second power demand is also shown in Figure 18.

Figure 18: Pressure Meter

The combined installation of the flowmeter and pressure gauge, designed to measure the second power demand originating from the oil pump and previously described in detail, along with their positioning on the vehicle, is shown in Figure 19.

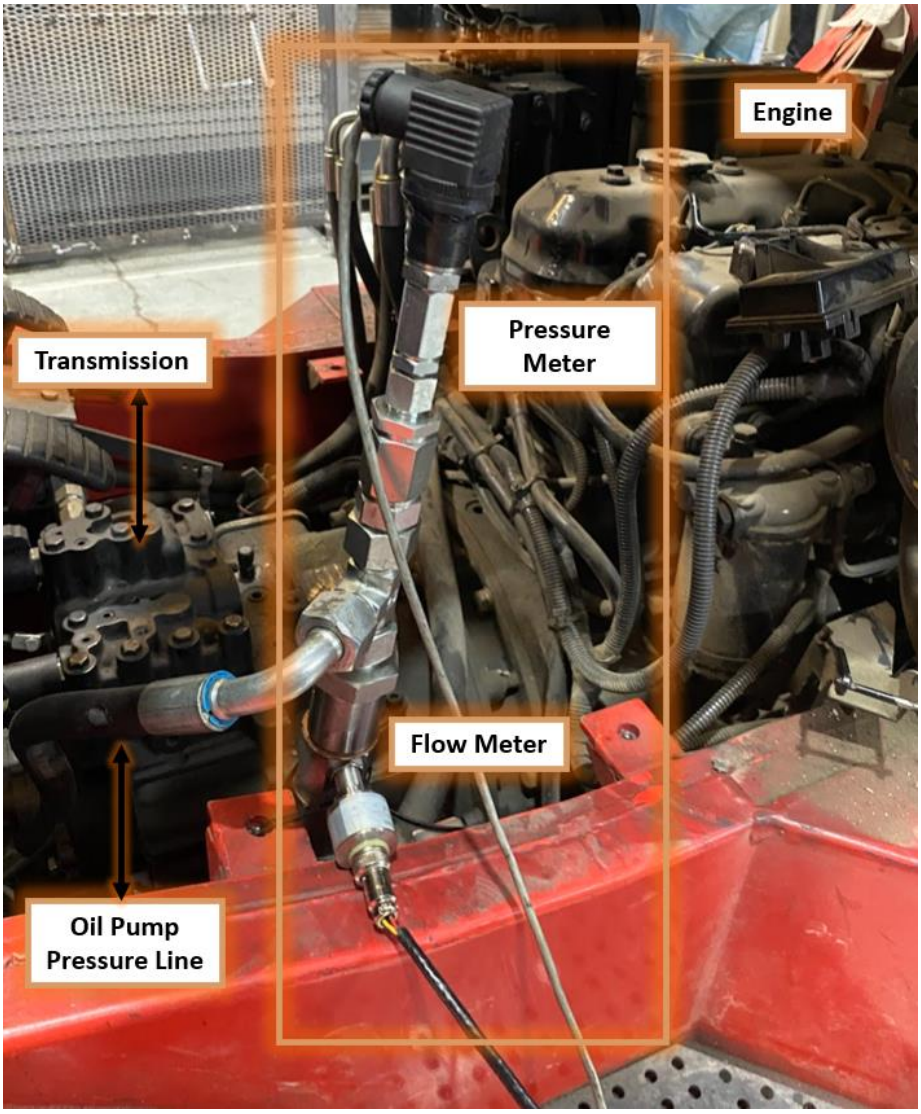

Figure 19: Location of Flow Meter and Pressure Meter

The IMU (Inertial Measurement Unit) device was positioned at the vehicle's center of gravity. Its location on the vehicle is shown in Figure 20. The IMU provides data on the vehicle's speed and position throughout the test cycle.

Figure 20: Installation of the IMU on the forklift truck

To ensure uninterrupted communication between the IMU and the GPS, the necessary antenna was installed on top of the forklift. The location of the antenna on the forklift is illustrated in Figure 21.

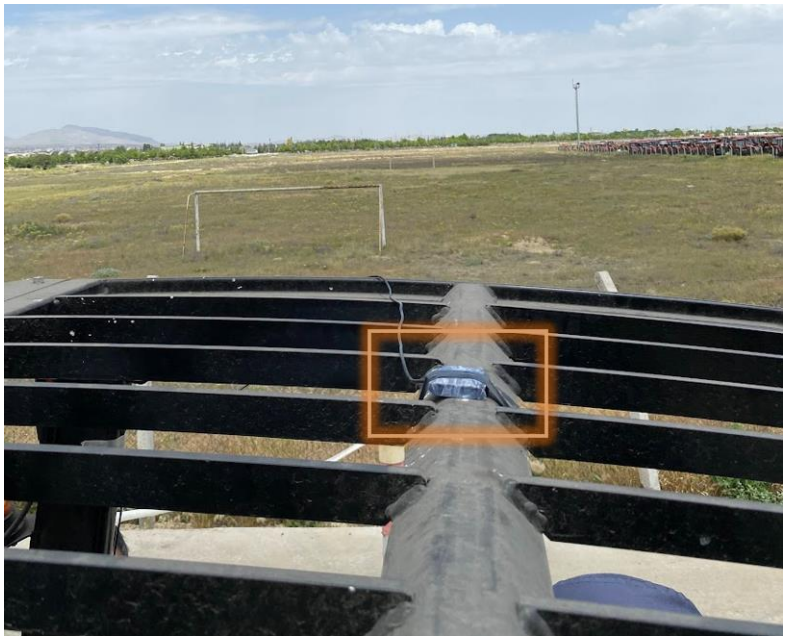

Figure 21: GPS Antenna of the IMU

The DEWE-43A device will be used to collect data from the sensors mentioned above. The DEWE-43A data acquisition system, shown in Figure 22, features 8 universal analog inputs, 8 digital/counter/encoder inputs, and two high-speed CAN bus inputs.

Figure 22: Dewe-43A Data Acquisition Device

In accordance with VDI 2198, the total fuel consumption at the end of the 60-minute test will be measured using an external fuel tank, which will serve as the fuel reservoir during the test. This tank is carefully filled at the start, and the amount of fuel consumed is determined at the end of the test. The position of the external fuel tank on the forklift is shown in Figure 23.

Figure 23: Position of External Fuel Tank on The Vehicle

The forklift, fully equipped with integrated test systems and loaded with the test weight for operation on the test track, is shown in a side view in Figure 24 and a rear view in Figure 25.

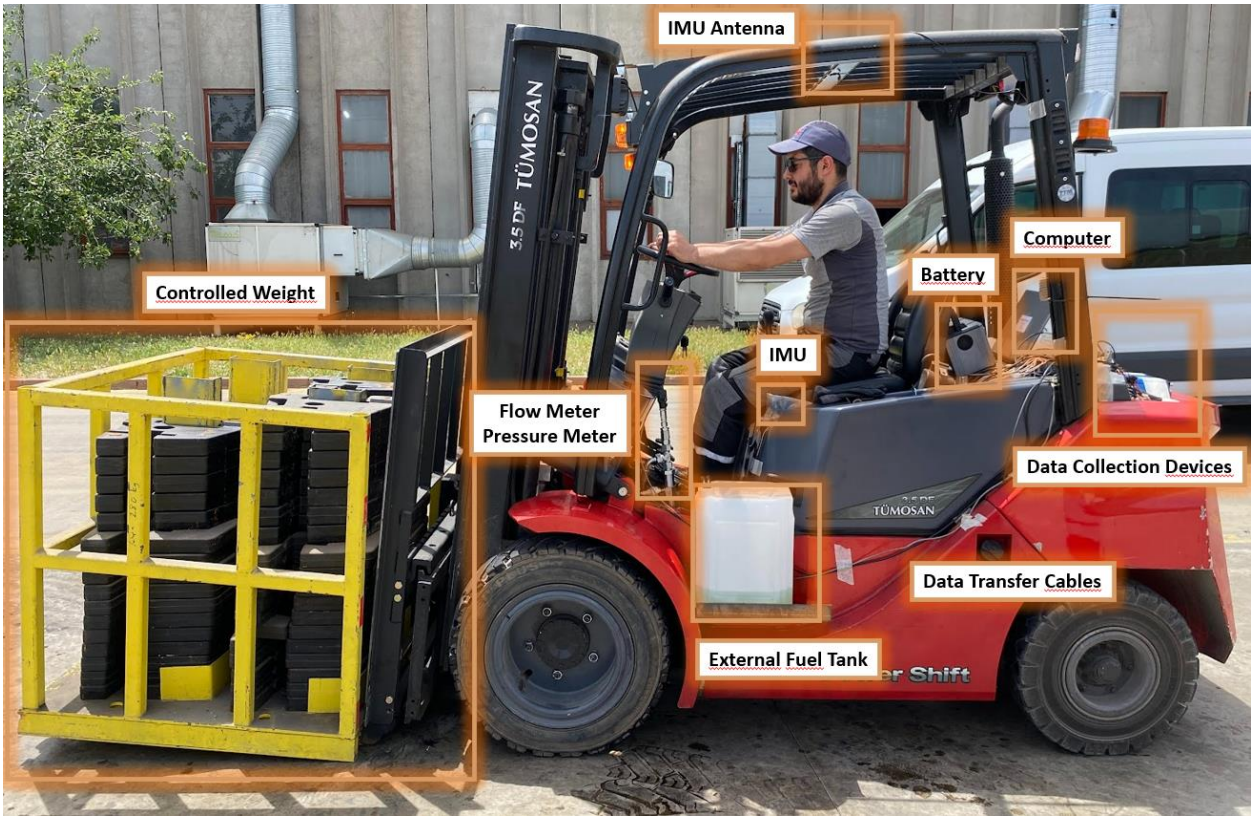

Figure 24: Side View of The Test Truck

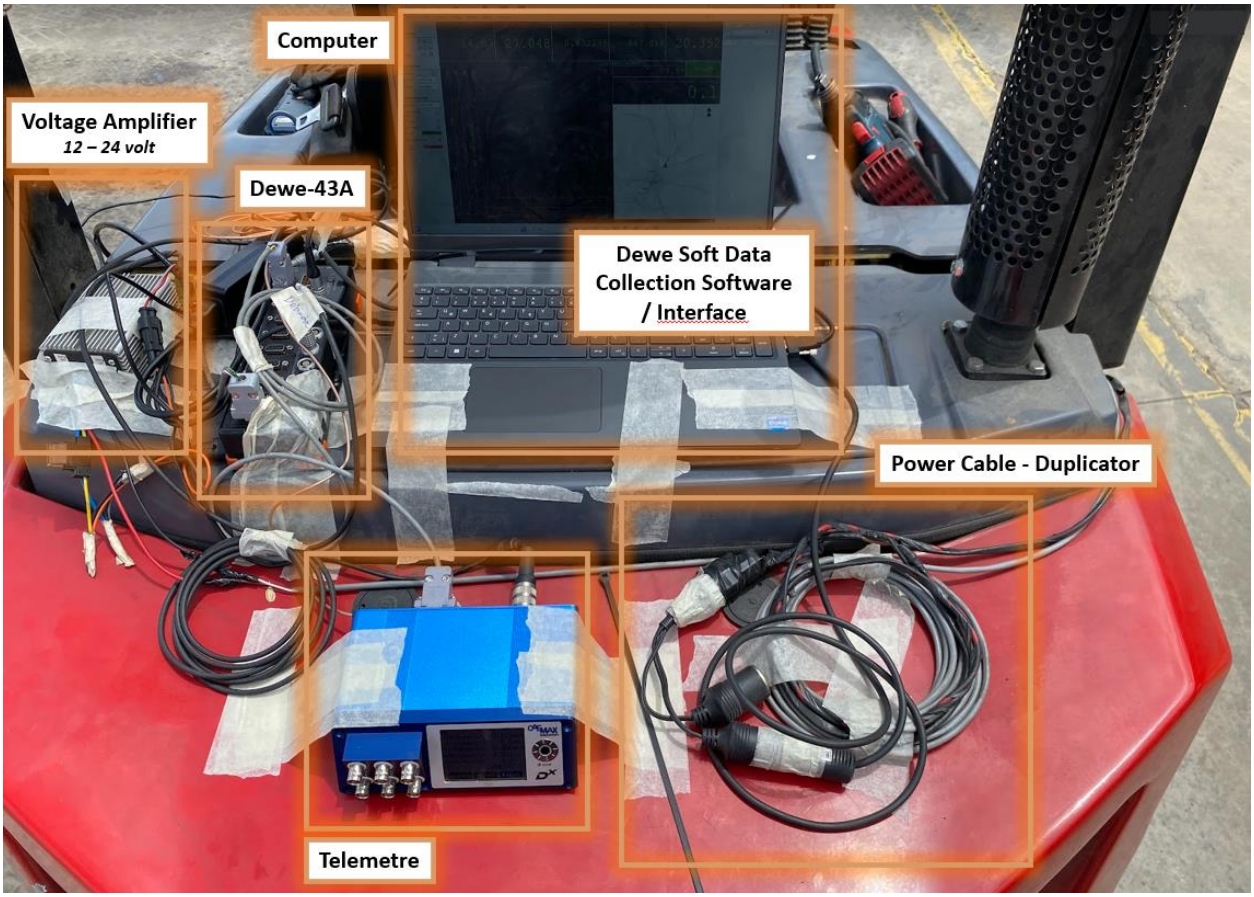

Figure 25: Rear View of The Test Truck

The test data screen, specifically designed for this test in the Dewesoft software, is shown in Figure 26. It enables real-time monitoring and recording of data collected from the sensors installed on the forklift during the test. The data transmitted to the interface include oil pump pressure, oil pump flow rate, hydraulic power, engine speed, engine torque, vehicle speed, and vehicle position.

Figure 26: Test Interface Screen Installed in Dewesoft Program

2.11. Test Results

In accordance with VDI 2198, the one-hour fuel consumption test determined that the forklift consumed 4.3 liters of fuel per hour, measured accurately using a calibrated container.

This test, comprising 3600 seconds and approximately 60 repetitions of a 60-second cycle, produced outputs that were nearly identical in each repetition.

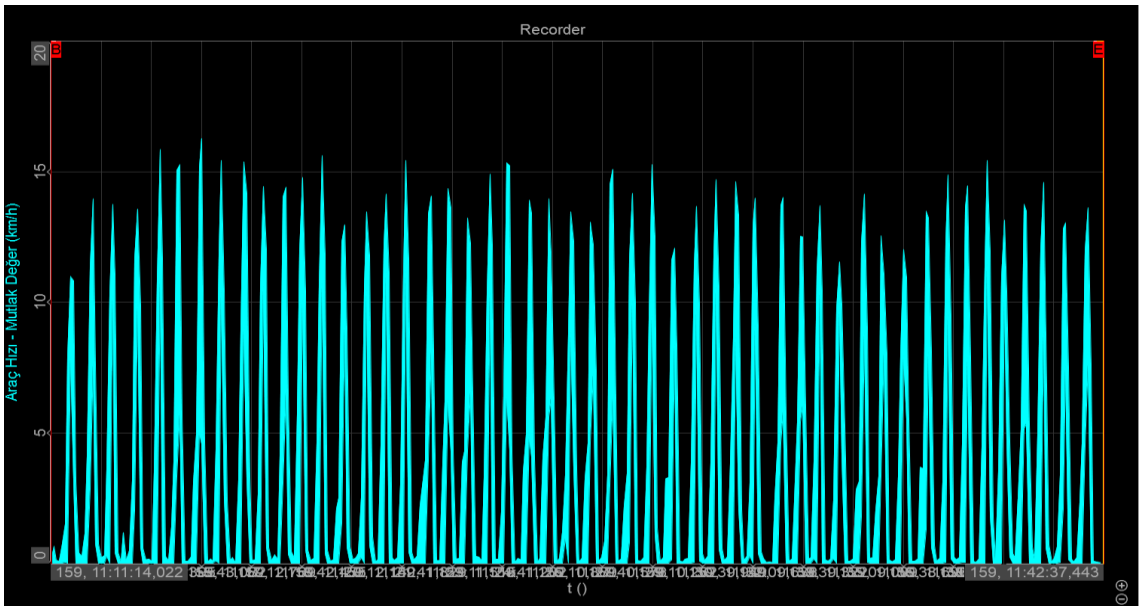

Figure 27: 3600 Seconds of Vehicle Speed vs Time Graph

Interpreting and analyzing data from the 3600-second test output shown in Figure 27 can be quite challenging. Therefore, Figure 28 presents a segment of the data corresponding to a single complete cycle, approximately 60 seconds in duration, for easier analysis and interpretation.

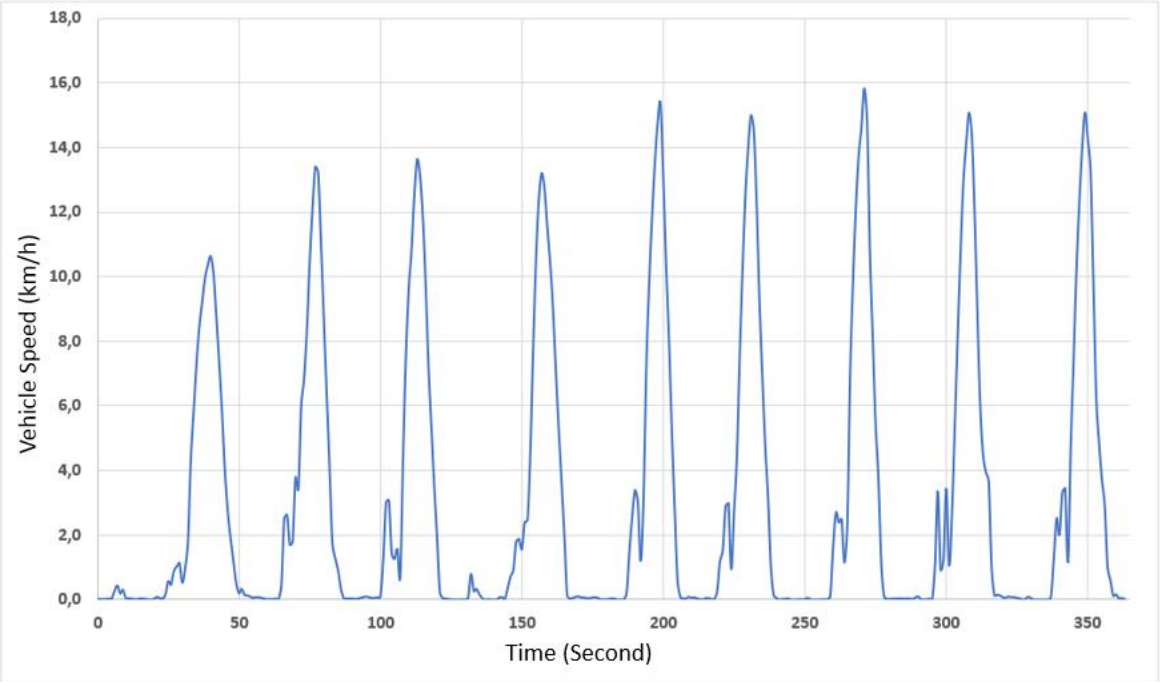

Figure 28: 360-Second Time-dependent vehicle speed graph

When examining the Time-Vehicle Speed graph, the movement patterns detailed in Figure 29 can be observed. These movement repetitions, corresponding to a complete cycle of approximately 60 seconds, continued with similar data patterns throughout the 60-minute duration of the test.

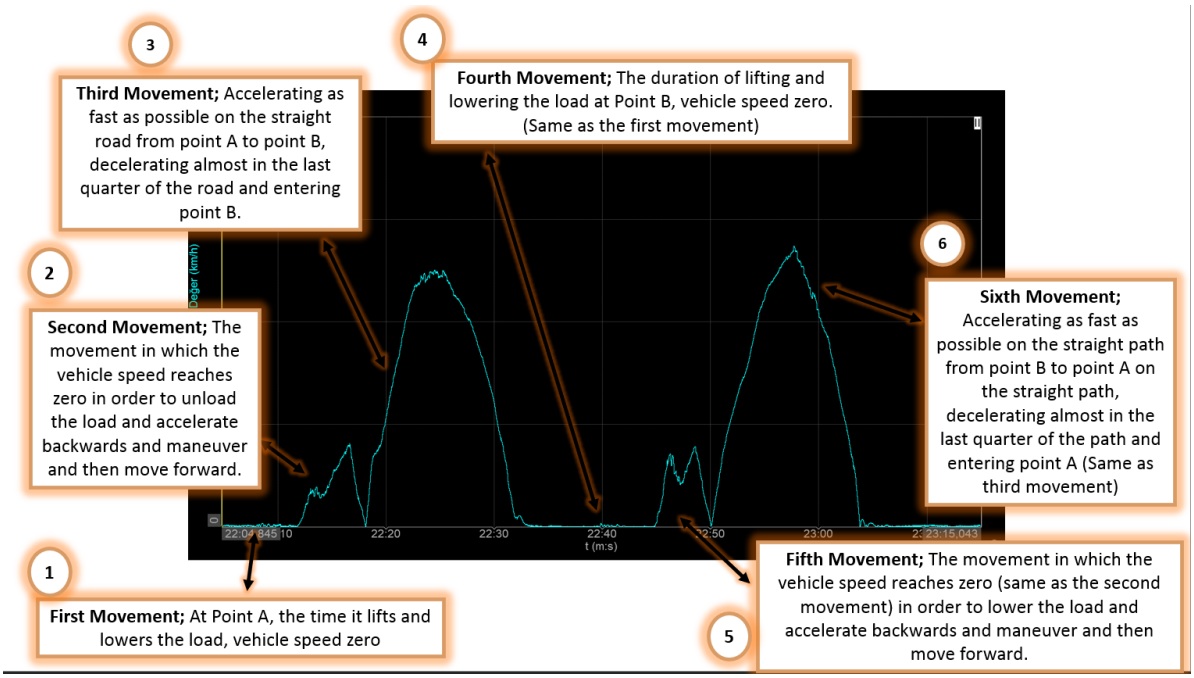

Figure 29: Interpretation of changing vehicle speed over one full lap (60 seconds)

Again for 60 seconds, the time domain variation of the total power, shown as the sum of the first and second power demands, is as shown in Figure 30.

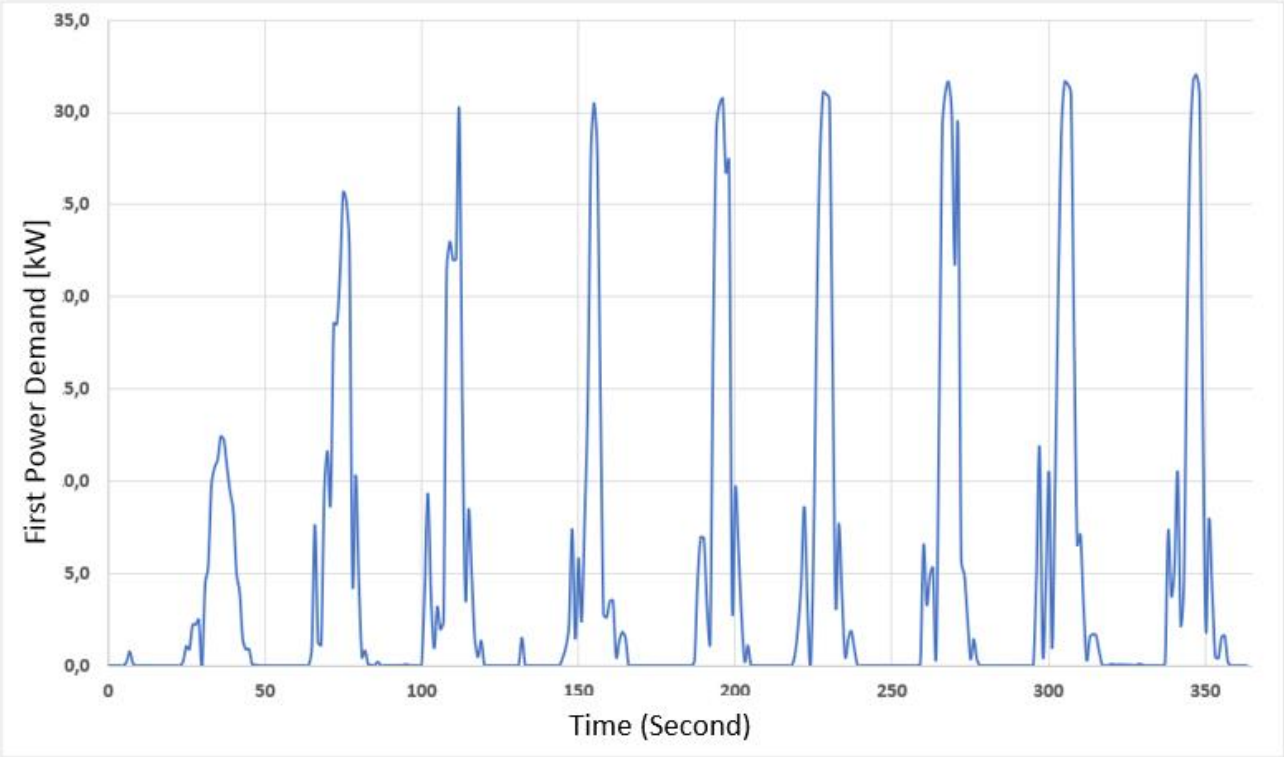

Figure 30: Time Dependent Power Graph

The time dependent engine speed graph is as shown in Figure 31.

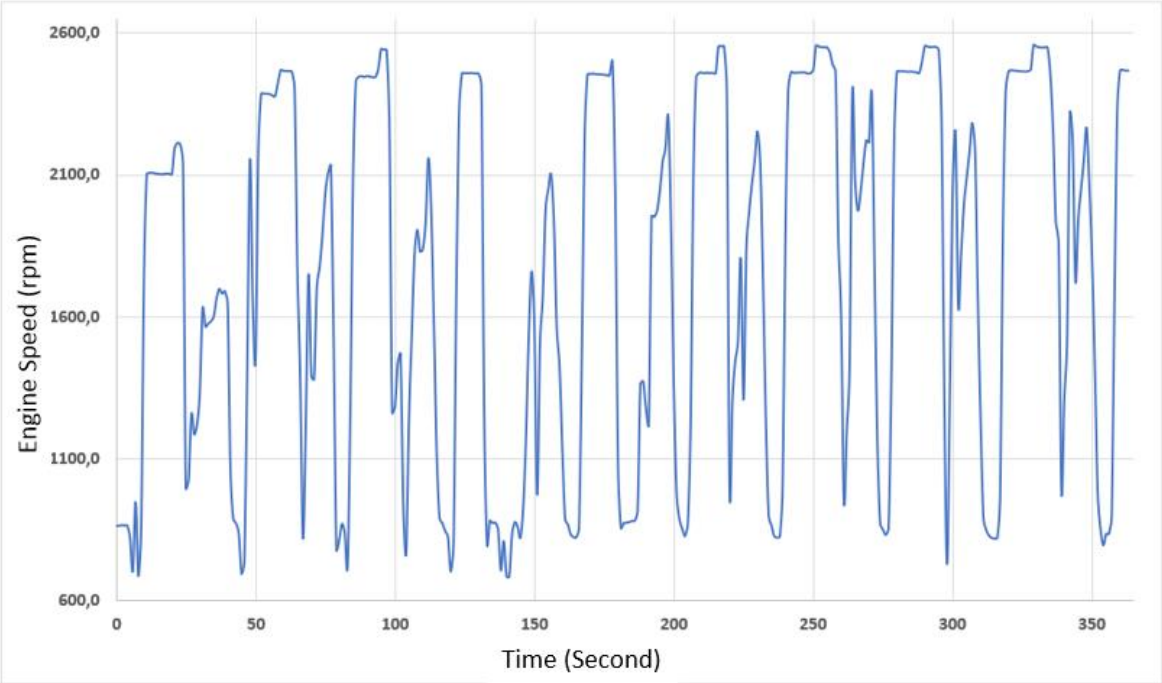

Figure 31: Time Dependent Power Graph

The time-dependent variation of the second power demand is as shown in Figure 32.

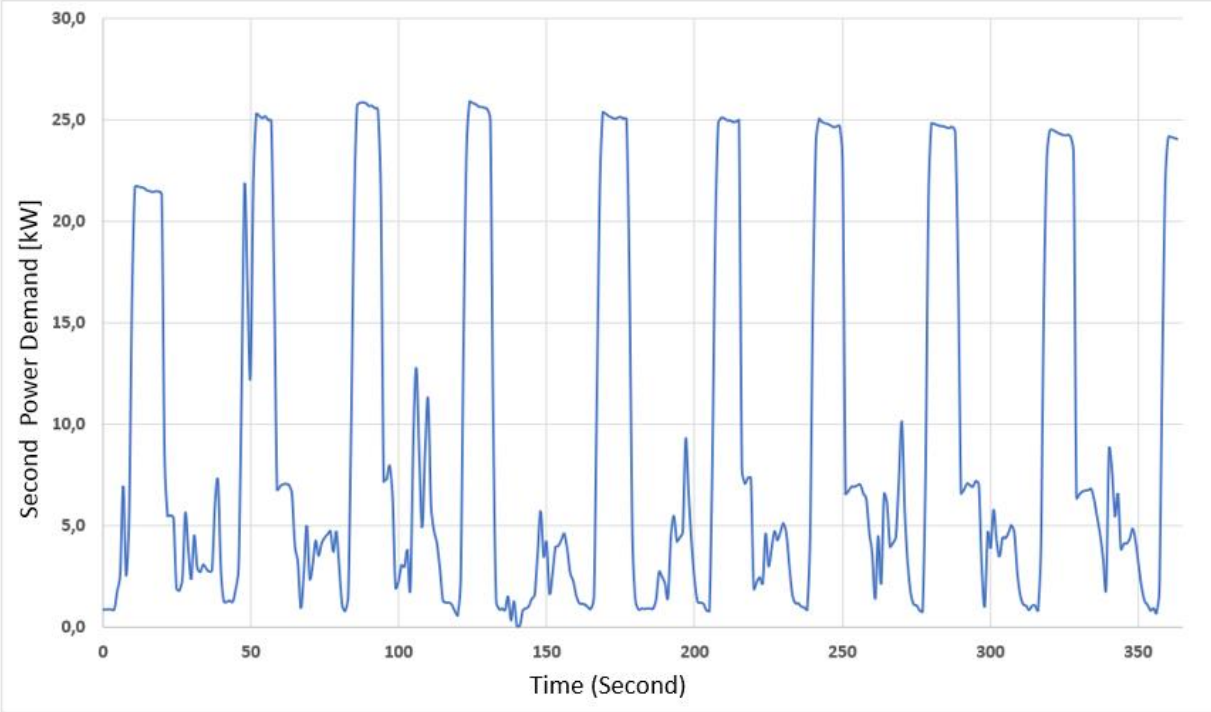

Figure 32: Time-Dependent Second Power Demand Graph

2.12. Vehicle Model

There are many pre-built software packages available for modeling vehicle fuel consumption and emissions. Some of the most commonly used include GT-Suite, MATLAB Simulink Simscape, AVL Cruise, and Adams Cars. In this study, the vehicle model will be developed directly using MATLAB programming language.

2.13. Systems to Model

The systems and their technical specifications, which were detailed in previous sections, will be modeled with the features outlined in the architecture shown in Figure 33.

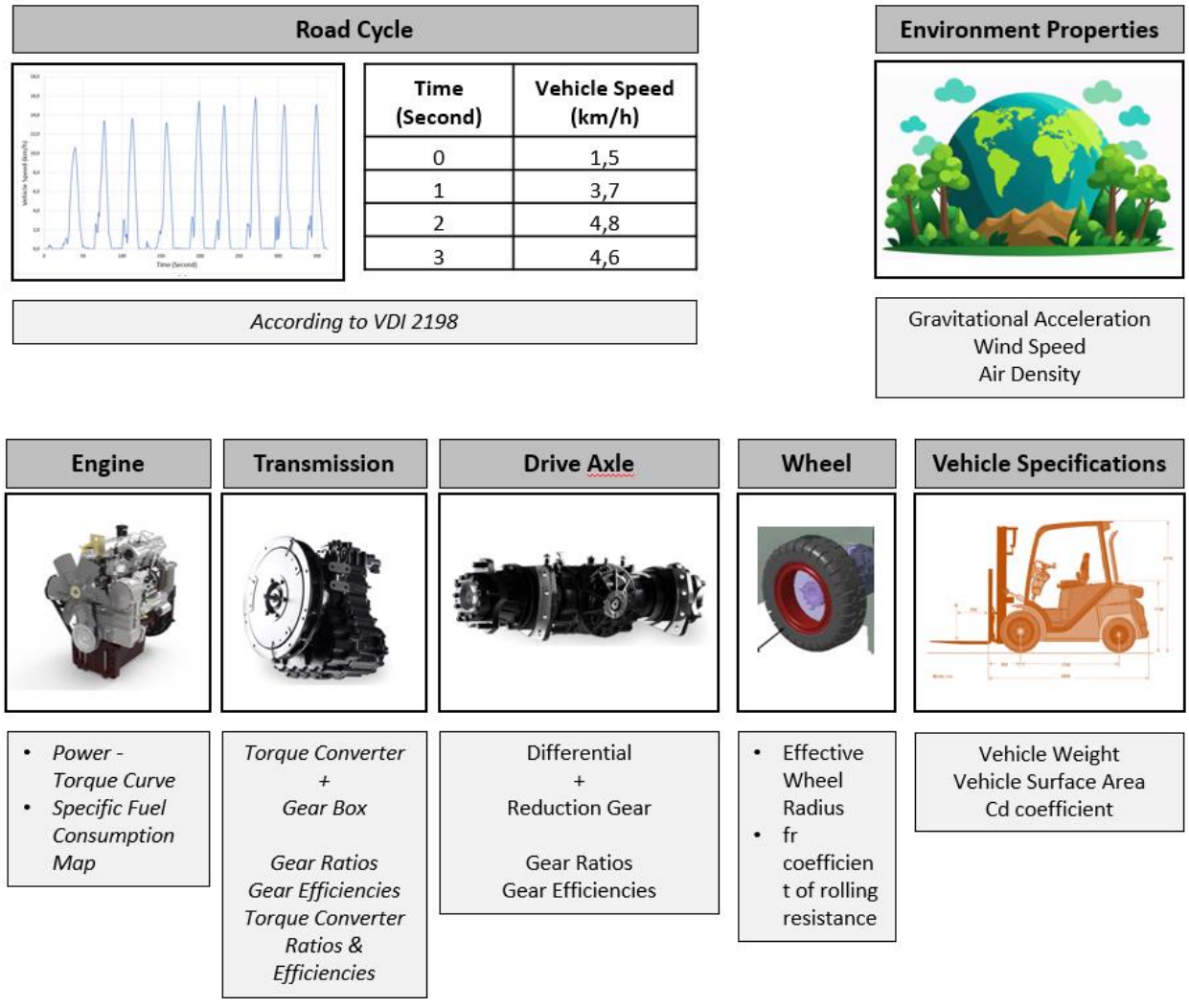

Figure 33: Summary View of The Systems to be Modeled

2.14. Algorithm

The step-by-step process of the algorithm, illustrated as a flow in Figure 34, is as follows:

- The characteristics of all systems shown in Figure 33, are predefined in the algorithm. A brief summary of these inputs is also provided in Figure 33.
- The duration of the cycle (number of rows/seconds to be processed) must be specified. For instance, the "63" input in Figure 34 indicates that the algorithm will calculate the cycle step by step up to the 63rd second (row). The "1:1:63" in Figure 33 means calculations will start at the 1st second (row) and proceed incrementally by 1 until the 63rd second (row).
- The algorithm is executed by pressing the "Run" command.
- Specified unit changes are applied.
- The vehicle speed at the 1st second (row) is accepted, and the resistances acting on the vehicle at that speed are calculated.
- The power demand required for the vehicle to overcome the resistances and maintain the expected speed in the cycle is determined.
- In the Torque Converter Modeling step, the torque curve provided by the torque converter is used to determine engine speed.
- Using the calculated engine speed and power demand, the specific fuel consumption map of the engine is utilized to determine the fuel consumed by the engine.
- These calculated values are stored as output for the 1st second (row).
- The algorithm checks whether the specified row (second) for calculation has been reached.
- If the specified row (second) has not been reached, the row number is incremented by 1, and the same calculations are repeated.
- If the specified row (second) has been reached, the calculations are terminated.
- Fuel consumption values calculated for each row (second) are summed to obtain the cumulative fuel consumption.
- These cumulative values are plotted over the time domain as outputs.

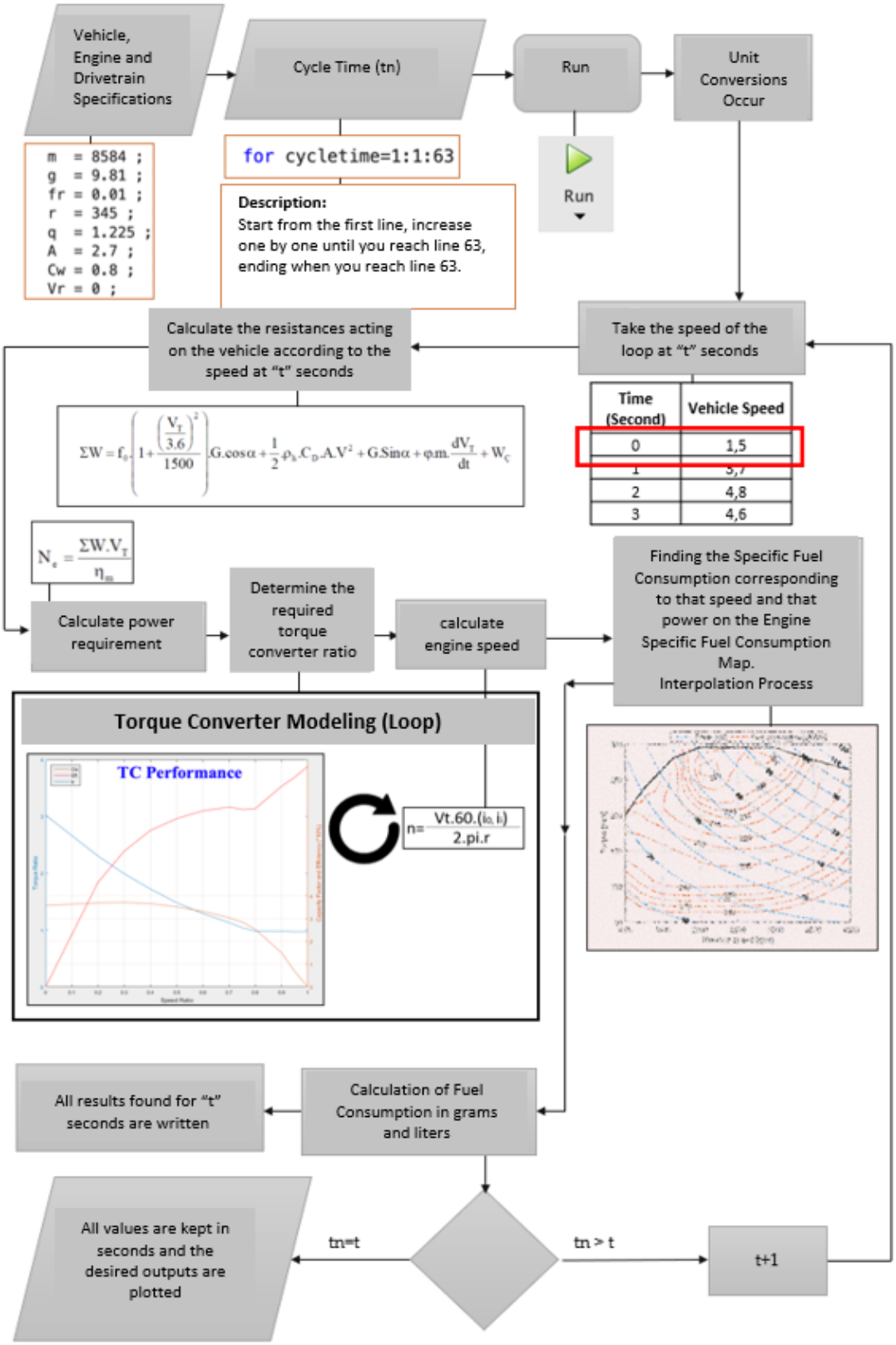

Figure 34: Algorithm Flow Diagram

In the resistance calculation section of the algorithm, as detailed in the relevant parts of the study, air resistance is disregarded since the vehicle's speed does not exceed approximately 20 km/h. According to the standard, the cycle must be conducted on a flat surface, and the tests were carried out accordingly. As a result, the forklift is not subjected to any grade resistance. Furthermore, since the forklift does not tow any trailers, vehicles, or similar loads, there is no towing resistance. In summary, the algorithm considers two types of resistance: rolling resistance and acceleration resistance.

In the detailed algorithm flow illustrated in Figure 34, the value represented as BeBe, found through interpolation from the engine's specific fuel consumption map based on power demand and required engine speed, is expressed in units of [g/kWh]. The value obtained from the specific fuel consumption map is multiplied by the instantaneous power and time, as shown in the following equation, to calculate the fuel consumption in grams. This value is then divided by the specific density of diesel fuel (0.836 kg/L) to convert it into liters, determining the amount of fuel consumed by the vehicle in that second.

$$B_E = \frac{N_e . B_e . hours}{836} \; [liter]$$

2.15. Program Outputs

The primary output of the 3600-second fuel consumption cycle, created in accordance with VDI 2198, is the fuel consumption value. As shown in Figure 35, the forklift consumed 3.94 liters of fuel during this cycle.

Figure 35: Summary Outputs Generated as a Result of The Cycle

The graph showing the variation of the engine speed in the time domain is shown in Figure 36.

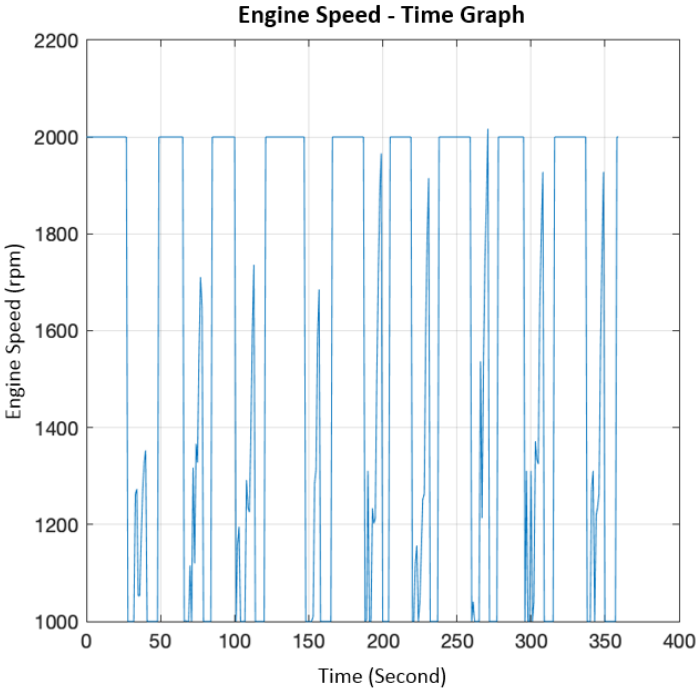

Figure 36: Time-based engine speed

The graph showing the power variation in the time domain is shown in Figure 35. In this graph, the first power demand is the power demand required for the truck to move forward.

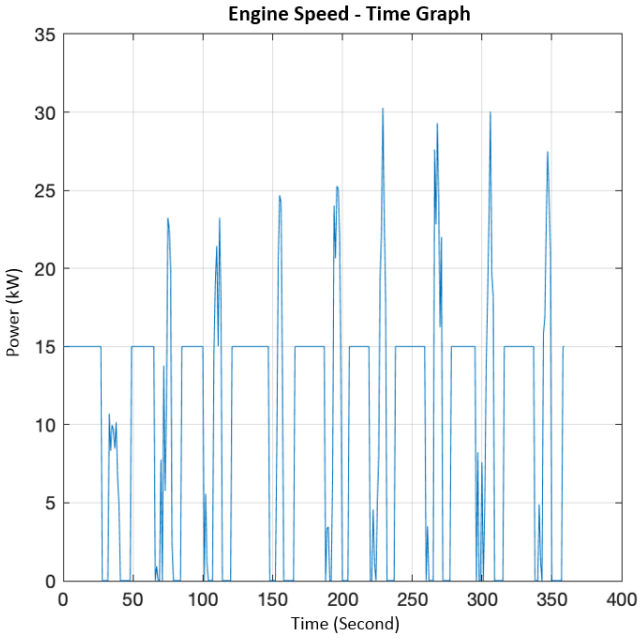

Figure 37: Time-dependent power demand

3. Results

Within the scope of this thesis, a Tümosan 3.5-ton diesel forklift was operated for 60 minutes on the fuel consumption test track specified in VDI 2198. Measurements were taken from an external fuel tank designed for the test to determine the total fuel consumed by the forklift during the cycle. Similarly, a model developed in MATLAB was run for a 60-minute test cycle, using the vehicle speed-time fuel consumption cycle from VDI 2198 test data as a reference. The program calculated the amount of fuel consumed during the cycle. A comparison between the fuel consumption measured during the test and the fuel consumption calculated by the MATLAB model is presented in Table 7 below.

Table 7: Traction Axle Characteristics

Test Result Fuel Consumption	4,3 lt / hour
Fuel Consumption Value of the Matlab model	3,9 lt / hour

There is an approximate 8% discrepancy between the actual test results and the MATLAB model outputs. The main reasons for this difference, listed in order of significance, are as follows: 1) Steering Power Consumption: The power required for steering is supplied by the hydraulic oil pump, but this steering function was not included in the MATLAB model. Since repeated left and right turns are performed during the cycle, this is considered the primary source of the difference between the test results and the model. 2) Cooling Fan Power: The power consumed by the cooling fan in the cooling system was neglected in the MATLAB model. 3) Alternator Power: The power consumed by the alternator was also excluded from the MATLAB model. 4) Wind Resistance: In the MATLAB model, wind resistance is passively calculated for speeds below 50 km/h. Since the forklift does not exceed 20 km/h during the cycle, this resistance was ignored. 5) Vehicle Surface Area: In the MATLAB model, the vehicle's surface area was calculated based on a general front perspective. However, the presence of a weight at the front of the forklift, which moves vertically, causes continuous changes in the effective surface area. 6) Tire Resistance: Due to the lack of technical information from the tire supplier and the absence of a specific rolling resistance coefficient test for the tires, a "Simple Tire Model" was used in the simulation. 7) Test Surface Variations: Although efforts were made to select the flattest possible area for the tests in the factory environment, minor surface irregularities and undulations that could affect resistance were present. 8) Mechanical Stability: Potential stability issues arising from the mechanical engine may have influenced the results. 9) Measurement Errors: Human errors could have occurred during the initial controlled fuel filling or while measuring the remaining fuel in the external test tank.

For future analysis studies, this observed discrepancy will be considered when evaluating the results. Incorporating the factors listed above into the simulation model will lead to more convergent results.

4. Discussion and Conclusion

There is an approximate 8% discrepancy between the actual test results and the MATLAB model outputs. The main reasons for this difference, listed in order of significance, are as follows: 1) Steering Power Consumption: The power required for steering is supplied by the hydraulic oil pump, but this steering function was not included in the MATLAB model. Since repeated left and right turns are performed during the cycle, this is considered the primary source of the difference between the test results and the model. 2) Cooling Fan Power: The power consumed by the cooling fan in the cooling system was neglected in the MATLAB model. 3) Alternator Power: The power consumed by the alternator was also excluded from the MATLAB model. 4) Wind Resistance: In the MATLAB model, wind resistance is passively calculated for speeds below 50 km/h. Since the forklift does not exceed 20 km/h during the cycle, this resistance was ignored. 5) Vehicle Surface Area: In the MATLAB model, the vehicle's surface area was calculated based on a general front perspective. However, the presence of a weight at the front of the forklift, which moves vertically, causes continuous changes in the effective surface area. 6) Tire Resistance: Due to the lack of technical information from the tire supplier and the absence of a specific rolling resistance coefficient test for the tires, a "Simple Tire Model" was used in the simulation. 7) Test Surface Variations: Although efforts were made to select the flattest possible area for the tests in the factory environment, minor surface irregularities and undulations that could affect resistance were present. 8) Mechanical Stability: Potential stability issues arising from the mechanical engine may have influenced the results. 9) Measurement Errors: Human errors could have occurred during the initial controlled fuel filling or while measuring the remaining fuel in the external test tank.

For future analysis studies, this observed discrepancy will be considered when evaluating the results. Incorporating the factors listed above into the simulation model will lead to more convergent results.

5. Acknowledge

Firstly, I extend my sincere gratitude to Mr. Orkun Özener for his invaluable support and encouragement throughout my academic journey. I would also like to express my heartfelt thanks to Mr. Mustafa Demir and Mr. Hüseyin Samet Kartal, whose collaboration and dedication have been instrumental in the development of new products and have greatly contributed to various stages of this study. Lastly, I wish to convey my

appreciation to the management and entire team at Tümosan Motor and Tractor Industry Inc. for providing the opportunity to bring these products to life and supporting academic pursuits.

References

[1] Eryiğit, O. (2024, May 15). Tumosan Forklift. Onur Eryiğit. Retrieved from https://www.onureryigit.com/portfolio-item/tumosan-forklift/

[2] Tümosan Motor ve Traktör A.Ş. (2024, May 15). Dizel Motor Kataloğu. Retrieved from https://www.tumosan.com.tr/tr/urunler/48hp

[3] Yamamoto, H., Harada, Y., & Hiraiwa, H. (2012). Introduction of hydrostatic transmission forklift model FH40-1/FH45-1/FH50-1. *Komatsu, ABD*, (No. 165).

[4] HD Hyundai XiteSolution. (2024, May 15). *Transmission Products*. Retrieved from https://www.hd-xitesolution.com/products/Transmissionp

[5] HD Hyundai XiteSolution. (2024, May 15). *Drive Axle Products*. Retrieved from https://www.hd-xitesolution.com/products/DriveAxle

[6] Yavaşlıol, İ. (2007). *Motor Vehicles – I*. Yıldız Teknik Üniversitesi Basım-Yayın Merkezi. ISBN: 9789754614299

[7] Verein Deutscher Ingenieure. (2012). *VDI 2198: International Standard*. VDI.

[8] Demir, M. (2024). Dizel motorlu ve tam elektrikli forkliftlerin çalışma parametreleri açısından kıyaslanması.